Journal of Engineering and Applied Sciences 13 (16): 6833-6843, 2018
ISSN: 1816-949X

PID Based Automatic Voltage Regulator Design for a Synchronous Generator Tuned Utilizing Particle Swarm Optimization under Different Damping Torque Coefficient

Mohanad Azeez Joodi
Department of Electrical Engineering, College of Engineering, University of Baghdad, Baghdad, Iraq

Abstract: In this study, the automatic voltage regulator for a synchronous generator has a been designed based on the Proportional Integral Derivative (PID) controller in which is tuned using the particle swarm optimization. The output voltage of the synchronous generator will be regulated, through the proposed structure and to check its effectiveness, another two controllers have been designed for comparison namely, unity closed loop system and pole placement method. The comparison shows that the step response performances under different values of the damping torque coefficients (settling time, peak value, overshoot percentage and steady-state error) was better when adopting the PID controller tuned using PSO. The bode plot measures (gain margin and phase margin) was also studied.

Key words: Automatic voltage regulator, PID controller, PSO and pole placement, gain margin

INTRODUCTION

The fundamental reason for the excitation system is to bolster the field twisting of the synchronous machine with the immediate current, so, the primary transition in the rotor is produced. Further, the terminal voltage of the synchronous machine is controlled by the excitation system appeared in Fig. 1 which additionally plays out various security and control errands, the central intention is to direct the terminal voltage and reactive power to maintain a strategic distance from shakiness of the creating station in a successful way (Kundur, 1994; Andersson, 2012).

An imperative part that PID controller tuning in the best possible working of the plant in which the controller is joined, the adjustment is done in the introduction strategy and is known as the two-arrange initialization (TSI), also in this technique can be understood that it causes the exciting algorithms to have more noteworthy

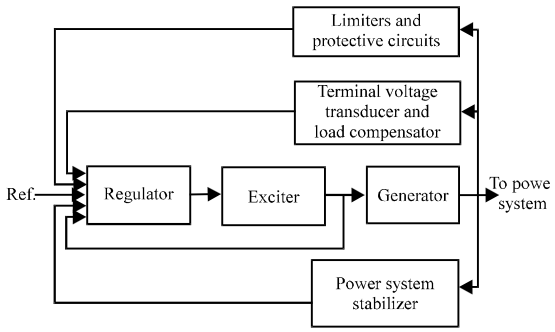

Fig. 1: Synchronous generator excitation control system (Andersson, 2012)

meeting rate and furthermore to unite at least estimation of the target capacities was lesser than another algorithm (Puralachetty *et al*., 2016). To control the Automatic Voltage Regulator (AVR) used a an integer order and fractional order corresponding in proportional plus integral plus derivative (IOPID) and (FOPID), the parameters of IOPID controller are tuned utilizing Ziegler-Nichols (ZN) method in utilizing the FOPID controller was enhanced the settling time of the system (Verma *et al*., 2015). Different controller outlined, for example, corresponding necessary derivative (PID) based on Adaptive Particle Swarm Optimization (APSO), PI, fuzzy PI and fuzzy PID for AVR as per it that fuzzy PID controller has a superior reaction than another controller, it discovered low ascent time and preferred execution over customary control (Khalid *et al*., 2016). Using Gravitational Search Algorithm (GSA) to plan an ideal PID controller for AVR and contrast it and different calculations, for example, GA found the best execution in GSA (Kumar and Shankar, 2015). Utilizing multi-objective non dominated sorting Genetic Algorithm 2 (NSGA-2) to outline and execution investigation of Proportional Integral Derivative (PID) controller for the AVR system and contrast it and alternate calculations, for example, Differential Evolutionary (DE) and Artificial Bee Colony (ABC). NSGA-2 is the advanced innovation which is reasonable to manage more than one target research all the while, likewise, manage vigor examination of the AVR system tuned by NSGA-2 calculation is performed by shifting the time constants of the amplifier, exciter, generator and sensor (Yegireddy *et al*., 2015). An ideal plan of the PID controller in the AVR system by utilizing Taguchi Combined Genetic Algorithm (TCGA) strategy,

a multi-target outline advancement to limit the greatest rate overshoot, the rise time, the settling time and the steady state error of the terminal voltage of the synchronous generator. By this technique will be tuned the proportional gain integral and derivative (PID) to control the AVR system for enhancing the step response of terminal voltage (Hasanien, 2013).

MATERIALS AND METHODS

Plant modeling: To investigate the effectiveness of using the Proportional Integral Derivative (PID) controller as a voltage regulator, the plant model which is the (exciter-generator) system is shown in Fig. 2. A numerical model for the exciter-generator plant was determined to rely on the swing equation perspective. The equation of focal significance in control system dependability examination is the rotational latency equation depicting the impact of unbalance between the electromagnetic torque and the mechanical torque of the individual machines. The standardized swing equation at that point can be communicated as two first order differential equations at that point:

$$\frac{d(\Delta\omega_r)}{dt} = \frac{1}{2H}(\bar{T}_m - \bar{T}_e - K_D\Delta\bar{\omega}_r) \quad (1)$$

$$\frac{d\delta}{dt} = \omega_o\Delta\bar{\omega}_r \quad (2)$$

The plant model will be introduced in the form of state space vector differential equation $\dot{x} = Ax+Bu$ (Buelna and Soto, 1997; Krohling *et al*., 1997). The V_{ref} and • P_m will be taken as inputs to the plant then:

$$\frac{d}{dt}\begin{bmatrix}\Delta\omega_r\\ \Delta\delta\\ \Delta E'\\ \Delta E_{fd}\end{bmatrix} = \begin{bmatrix}\frac{-K_D}{2H} & \frac{-K_1}{2H} & \frac{-K_2}{2H} & 0\\ \omega_o & 0 & 0 & 0\\ 0 & \frac{-K_3K_4}{T_3} & \frac{-1}{T_3} & \frac{K_3}{T_3}\\ 0 & \frac{-KAK_5}{T_E} & \frac{-KAK_6}{T_E} & \frac{-K_E}{T_E}\end{bmatrix} \quad (3)$$

$$\begin{bmatrix}\Delta\omega_r\\ \Delta\delta\\ \Delta E'\\ \Delta E_{fd}\end{bmatrix} + \begin{bmatrix}\frac{1}{2H} & 0\\ 0 & 0\\ 0 & \frac{KA}{T_E}\\ 0 & \end{bmatrix}\begin{bmatrix}\Delta P_m\\ V_{ref}\end{bmatrix}$$

Then from Eq. 3:

$$[A] = \begin{bmatrix}\frac{-K_D}{2H} & \frac{-K_1}{2H} & \frac{-K_2}{2H} & 0\\ \omega_o & 0 & 0 & 0\\ 0 & \frac{-K_3K_4}{T_3} & \frac{-1}{T_3} & \frac{K_3}{T_3}\\ 0 & \frac{-KAK_5}{T_E} & \frac{-KAK_6}{T_E} & \frac{-K_E}{T_E}\end{bmatrix} \text{ and } [B] = \begin{bmatrix}\frac{1}{2H} & 0\\ 0 & 0\\ 0 & \frac{KA}{T_E}\end{bmatrix}$$

For the normal AVR, the state space efficiency can be self-determined, for the model of Eq. 3, the terminal voltage is taken as a yield and can be given as:

$$\Delta E_t = K_5\,\Delta\delta + K_6\,\Delta E' \quad (4)$$

or in a matrix form:

$$\Delta E_t = \begin{bmatrix}0 & K_5 & K_6 & 0\end{bmatrix}\begin{bmatrix}\Delta\omega_r\\ \Delta\delta\\ \Delta E'\\ \Delta E_{fd}\end{bmatrix} \quad (5)$$

The transfer function of the open loop system is:

$$TF = \frac{2.033s^2+0.8713s+97.39}{s^4+0.8478s^3+36.5s^2+7.727s+97.36} \quad (6)$$

Pole placement algorithm: Have the usual way with the contour of the Single Input Single Output (SISO) control regulator system (controller) to make that closed loop dominant poles a desirable damping ratio z and a natural frequency of w_n undamped natural freq. The unipolar placement method has all closed loop poles (there are costs associated with the implementation of all closed-loop poles, however, since, setting all loop poles requires a successful estimation of all state variables).

Such a system in which the reference input constantly has zeros is known as a control system. A schematic diagram of this system is illustrated in Fig. 3. The problem of adjusting the control poles (closed loop poles) in the coveted area is called the unipolar placement problem and this should be possible if and only if the system indicates that it is fully controllable. In this approach, the system requirement can be increased by 1 or 2 unless a pole-zero erase occurs. Note that in this approach, we expect that the consequences of the reactions of the closed uncontrolled poles are unimportant. Not quite equivalent to the determination of existing closed-loop poles (the usual plan approach), the current pole shift approach indicates all closed poles. There are costs associated with the development of all closed-loop poles, depending on whether the control loop

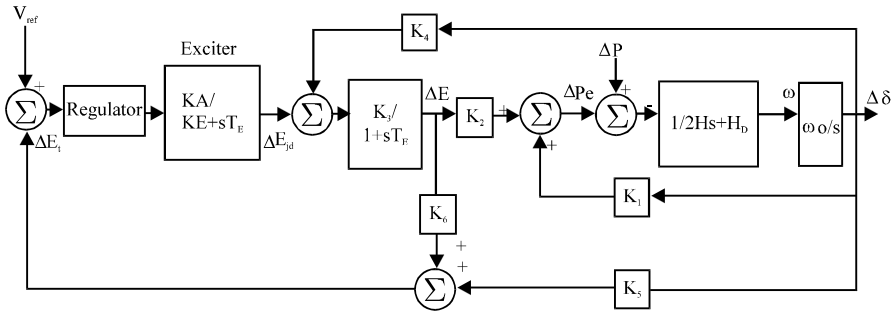

Fig. 2: Exciter generator model

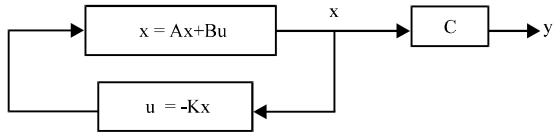

Fig. 3: Pole placement block diagram

setting requires a successful estimation of all state factors or the inclusion of a state observer is necessary for the system. There is also the need for the system to place the closed poles in the auto-trigger zone to have (Khalid *et al*., 2016; Kumar and Shankar, 2015; Yegireddy *et al*., 2015; Tuaimah *et al*., 2014). The suggested poles that can enhance the system performance has been chosen to be as: -0.4706+0.5228i, -0.4706-0.5228i, - 9.4118+10.4565i, -9.4118-10.4565i base with these poles the controller transfer function will be.

$$TF = \frac{2.033s^2+0.8713s+97.39}{s^4+19.76s^3+216.1s^2+195.6s+97.93} \quad (7)$$

PID controller design: A Proportional-Integral-Derivative control device (PID regulator or three-term regulator) is generally used in modern control systems and a variety of different applications requiring continuous control optimized a closed-loop feedback instrument. A PID regulator continuously calculates an error value e (t) as the difference between a desirable target value (SP) and a deliberate Process Variable (PV) and applies an adjustment to proportional integral and derivative terms. (named P, I and D individually) which give the name of the controller. both the scientific model and the reasonable loop above use a "direct" control activity for each of the terms, implying that a positive spread error causes a relentlessly positive control income for summer conditions to apply the cure. The general form of a PID regulator, showing the 3 expressions mentioned above can be given by the following algorithm: (:kp = 1.2749, ki = 0.7918 and kd = 5.3238) at K_D = 3 in Fig. 4. And the general transfer function can be given as in follows:

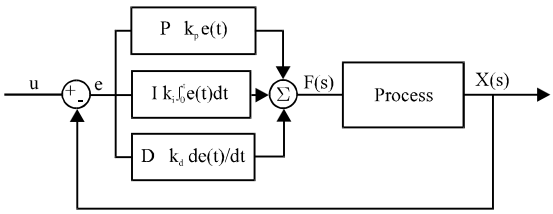

Fig. 4: PID algorithm

$$TF = \frac{0.5412s^4+0.3615s^3+26.06s^2+6.242s+3.856}{s^5+1.389s^4+3.493s^3+32.96s^2+11.90s+3.856} \quad (8)$$

$$u(t) = K_p e(t)+K_i \int_0^t e(t)dt+K_d \frac{de(t)}{dt}$$

In any case, the yield is called "reverse" acting if it's important to apply negative restorative activity (Ogata, 2010).

Particle swarm optimization: These algorithms impersonate the social conduct of winged birds running. Beginning to frame a haphazardly disseminated set of particles (potential arrangements), the calculations attempt to enhance the arrangements as indicated by a quality measure (wellness research). The spontaneous creation is performed by moving the particles around the inquiry space by methods for an arrangement of straightforward scientific articulations which display some antiparticle interchanges. These numerical articulations in their least complex and most fundamental shape, propose the development of every molecule toward its own best-experienced position and the swarm's best position up until this point, alongside some irregular annoyances. There is a wealth of various variations utilizing distinctive refreshing standards, notwithstanding. The thought was to at first create an arrangement of focuses and to allow an underlying speed vector to each of them. Utilizing these speed vectors, every molecule changes its position iteratively while the speed vectors are being balanced by some irregular components:

$$\left(V_{i,j}\right)^{k+1} = \left(V_{i,j}\right)^{k} + C_1 r_1 \left(\left(Xbest_{i,j}\right)^{k} - \left(X_{i,j}\right)^{k}\right) + C_2 r_2 \left(\left(Xgbest_{j}\right)^{k} - \left(X_{i,j}\right)^{k}\right) \quad (9)$$

$$\left(X_{i,j}\right)^{k+1} = \left(X_{i,j}\right)^{k} + \left(V_{i,j}\right)^{k+1} \quad (10)$$

where $(x_{i,j})^k$ and $(v_{i,j})^k$ are the jth segment of the ith molecule's position and speed vector, separately in the kth emphasis, r1 and r2 are two irregular numbers consistently disseminated in the range (1, 0), xbesti and xgbest demonstrate the best positions experienced, so far by the ith molecule and the entire swarm, separately and c1 and c2 are 2 parameters speaking to the molecule's trust in itself (cognizance) and in the swarm (social conduct) individually (Rao, 2009).

Particle swarm optimization are designed to solve the PID controller to get the best value of errors (g_best value = 0.0204) and get the best values of P, I and D(kp = 1.2749, ki = 0.7918 and kd = 5.3238) when the damping torque coefficient K_D = 3. Table 1 shows PSO settings and initial conditions used. Accordingly the transfer function of PID controller will be:

$$TF = \frac{5.324s^2 + 1.275s + 0.7918}{s} \quad (11)$$

Table 1: Parameters for the PSO algorithm

PSO settings	Values
Particles No.	25
Swarm No.	3
Iteration No.	150
C1, C2	1.1
W	0.729
Kp	0-7
Ki	0-3
Kd	0-20

RESULTS AND DISCUSSION

Performance evaluation of design conventional AVR: The algorithms discussed in the previous sections are applied to the terminal voltage exciter of the synchronous generator as AVR and to demonstrate the efficiency of the PID regulator, it is checked with a feedback controller and a pole placement controller with K_D = 3. Figure 5 and 6 show the results of applying the unity feedback as a controller on the exciter, namely the step response, bode plot respectively. Figure 7 and 8 show the results of applying the PID with PSO tuning as a controller on the exciter, namely the step response, bode plot, respectively. Figure 9 shows the results of applying the pole placement technique as a controller on the exciter, namely the step response. Figure 10 shows the results of applying the Unity feedback, PID with PSO tuning and pole placement technique as a controller on the exciter, namely the step response, bode plot, respectively. Table 2 shows the step response performance when designing the controller at K_D = 3, Table 3 shows the gain margin and phase margin for the same damping torque coefficient. When K_D = 6 it can be found that the three terms of the PID controller after tuning with PSO algorithm and after 150 iterations (kp = 1.3973, ki = 0.8630 and kd = 5.9190). The above cases are shown in Fig. 11-16. Table 4 shows the step response performance when designing the

Table 2: The performance of system when applied the controller at K_D = 3

Controller	Peak value	Overshoot (%)	Rise time (sec)	Settling time (sec)	Steady state error
Unity feedback system	1.87	86.80	0.605	44.60	0
System with pole placement	1.05	05.85	2.92	8.64	0.006
System with PID controller	1.01	01.28	2.51	3.82	0

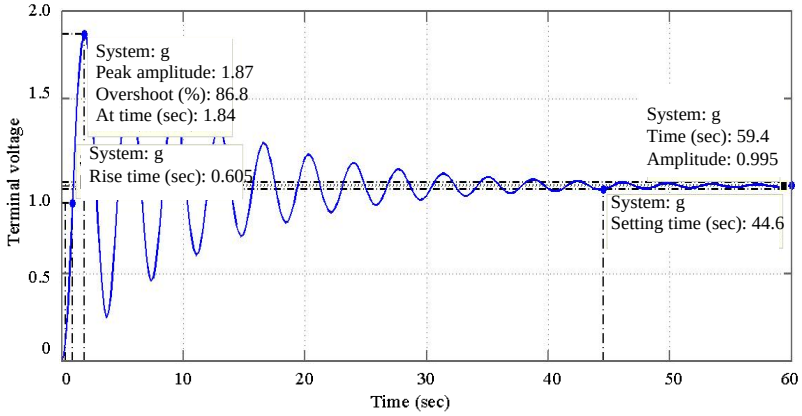

Fig. 5: Terminal voltage with unity feedback; AVR characteristic when system is closed loop

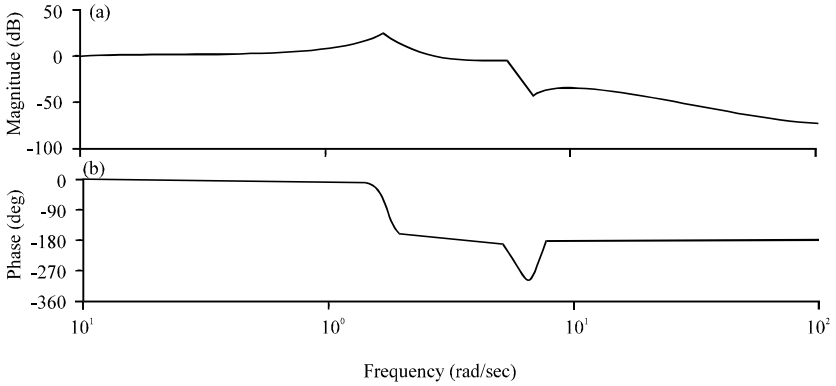

Fig. 6ab): Bode plot of the open loop system; Gm = 8.47 dB (at 3.44 rad/sec), Pm = 5.81 deg. (at 2.44 rad/sec)

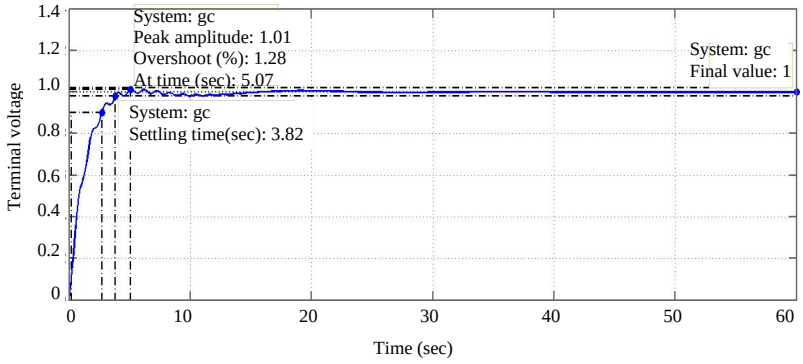

Fig. 7: Terminal voltage with AVR designed as PID controller; AVR characteristic when system with controller PID

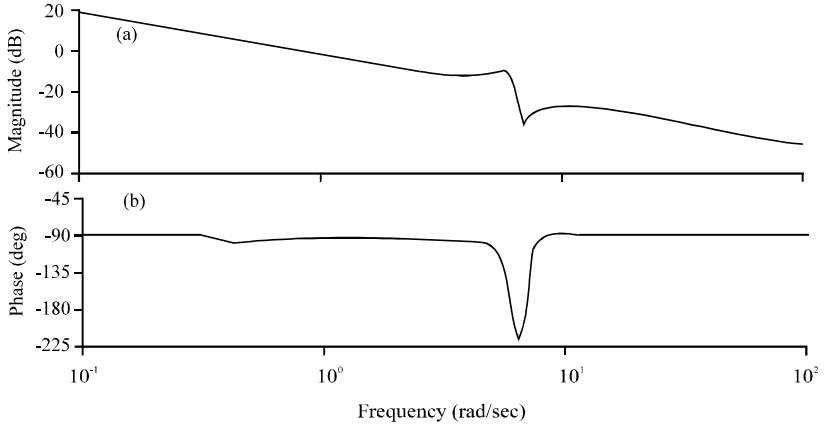

Fig. 8ab): Bode plot with AVR designed as PID controller on open loop

Table 3: The gain margin and phase margin of two cases at $K_D = 3$

Controller types	Gm (dB)	Wgm (rad/sec)	Pm (deg.)	Wpm (rad/sec)
Open loop system	8.47	3.44	5.81	2.440
Open loop system with PID controller	10.30	5.92	85.70	0.766

Table 4: The performance of system when applied the controller ($K_D = 6$)

Controller types	Peak alue	Overshoot (%)	T_r (sec)	T_s (sec)	T_{sse} (sec)
Unity feedback system	1.88	87.900	0.611	48.00	0.000
System with pole placement	1.05	5.850	2.930	8.63	0.006
System with PID controller	1.01	0.574	2.400	3.75	0.000

controller at $K_D = 6$, Table 5 shows the gain margin and phase margin for the same damping torque coefficient.

When $K_D = 0$ it can be found that the three terms of the PID controller after tuning with PSO algorithm and after 150 iterations (kp = 0.5898, ki = 0.4317 and kd = 2.8757). The above cases are shown in Fig. 17-22. Table 6 shows the step response performance when designing the controller at $K_D = 0$, Table 7 shows the gain margin and phase margin for the same damping

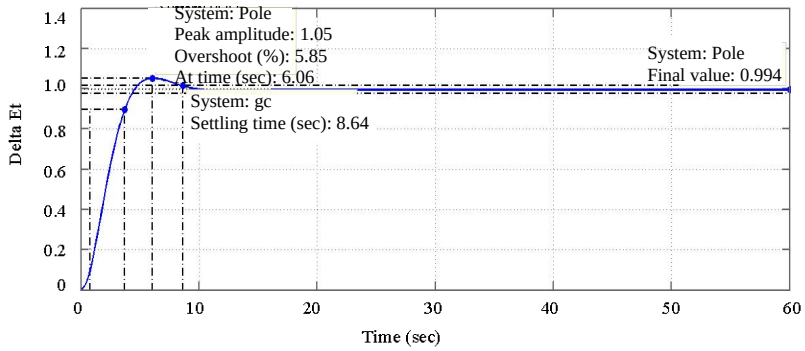

Fig. 9: Terminal voltage with AVR designed as pole placement controller

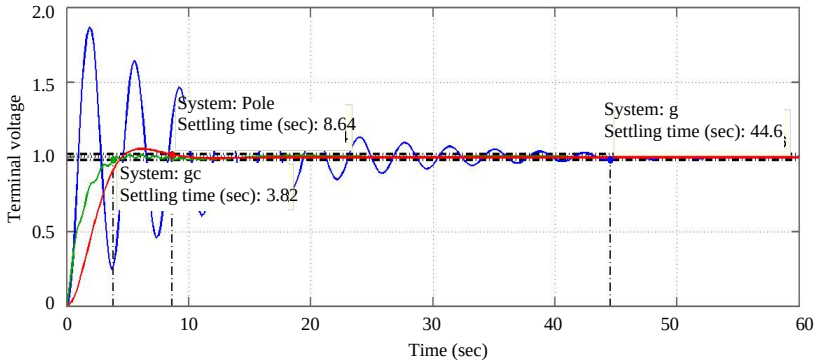

Fig. 10: Step response characteristics with closed loop, PID controller and pole placement

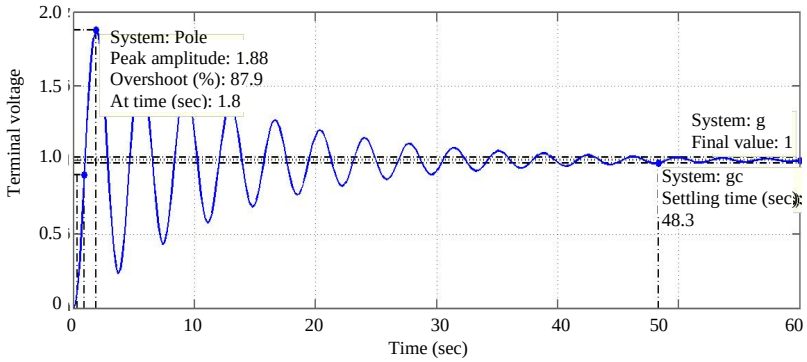

Fig. 11: The unity feedback system with $K_D = 6$

Table 5: The gain margin and phase margin of two cases at $K_D = 6$

Controller types	Gm (dB)	Wgm (rad/sec)	Pm (degree)	Wpm (rad/sec)
Open loop system	6.37	3.09	4.5	2.44
Open loop system with PID controller	16.50	6.15	86.2	0.85

Table 6: The performance of system when applied the controller at $K_D = 0$

Controller types	Peak value	Overshoot (%)	T_r (sec)	T_s (sec)	T_{ss}(sec)
Unity feedback system	1.86	85.700	0.599	42.50	0.000
System with pole placement	1.05	5.850	2.920	8.65	0.006
System with PID controller	1.01	0.925	4.870	7.99	0.000

Table 7: The gain margin and phase margin of two cases at $K_D = 0$

Controller types	Gm (dB)	Wgm (rad/sec.)	Pm (Degree)	Wpm (rad/sec)
Open loop system	11	4.04	7.17	2.45
Open loop system with PID controller	5.46	5.85	84	0.41

torque coefficient (Fig. 16-22). The comparative study for the unity feedback system and open loop system for the three damping torque coefficient ($K_d = 0$, $K_d = 3$ and $K_d = 6$) are shown in Table 8 and 9. The

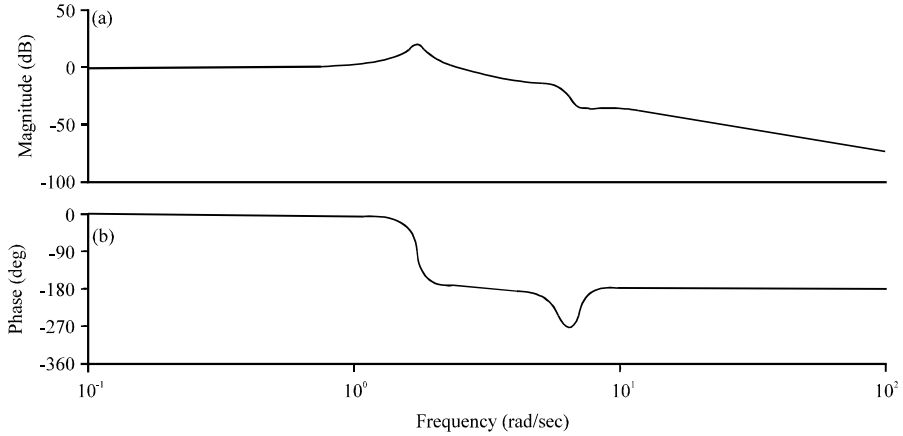

Fig. 12ab): The bode diagram of the open loop system with (K_D = 6)

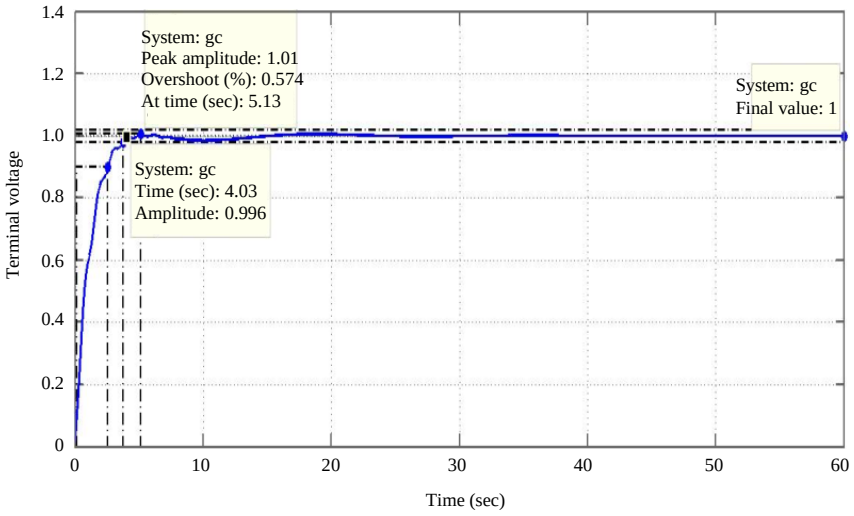

Fig. 13: The step response of the PID controller with system (K_D = 6); Gm = 6.37 dB (at 3.09 rad/sec), Pm = 4.5° (at 2.44 rad/sec)

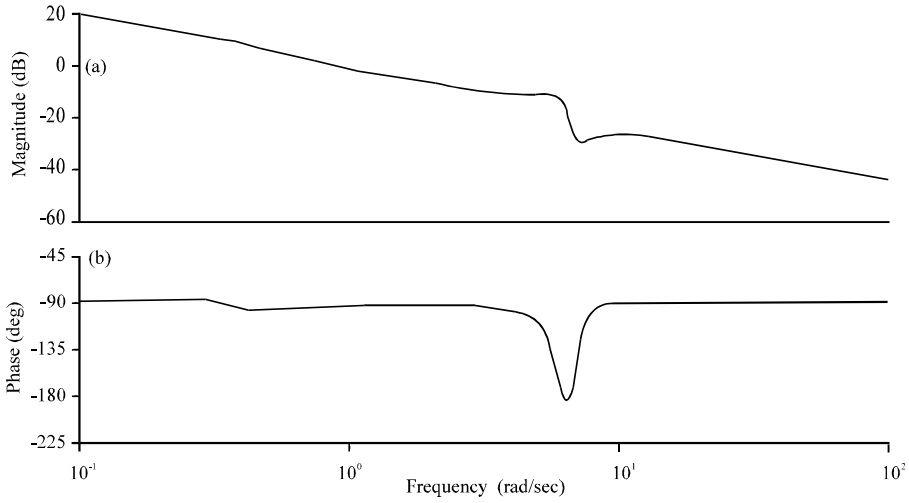

Fig. 14ab): The bode diagram of the PID with system open loop (K_D = 6)

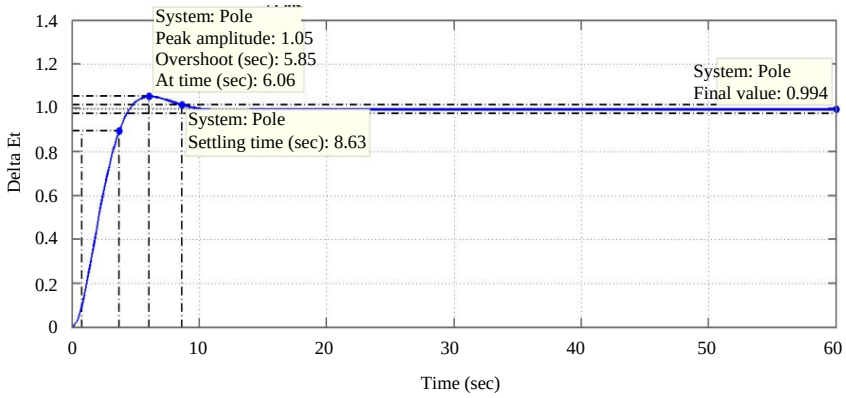

Fig. 15: The pole placement step response (K_D = 6)

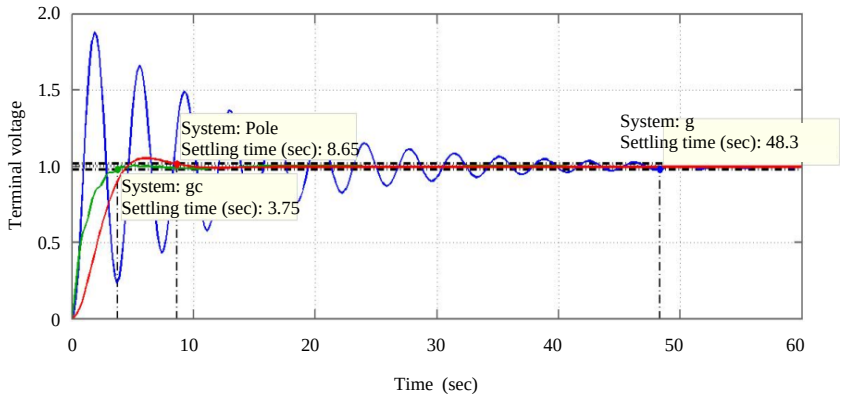

Fig. 16: The three-step responses with (K_D = 6)

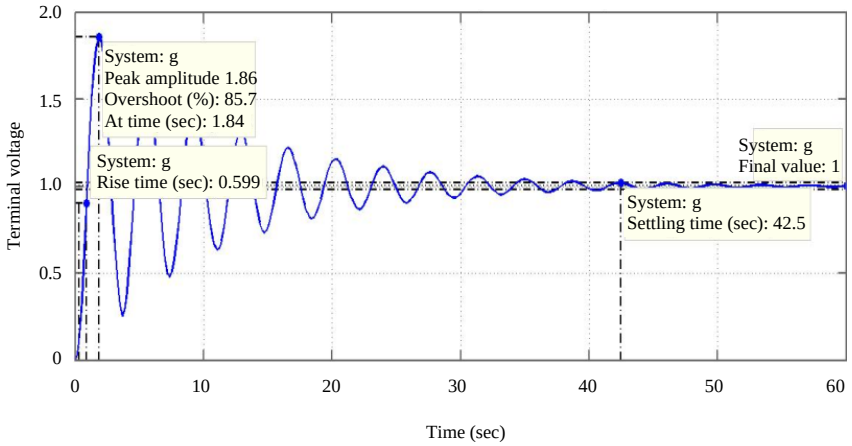

Fig. 17: The unity feedback system with K_D = 0

Table 8: The performance of system for the unity feedback with three cases of K_D

K_D	Controller type	Peak value	Overshoot (%)	T_r (sec)	T_s(sec)	T_{ss} (sec)
0	Unity feedback system	1.86	85.7	0.599	42.5	0
3	Unity feedback system	1.87	86.8	0.605	44.6	0
6	Unity feedback system	1.88	87.9	0.611	48	0

Table 9: The gain margin and phase margin for the open loop system with three cases of K_D

K_D	Controller	Gm (dB)	Wgm (rad/sec)	Pm (degree)	Wpm (rad/sec)
0	Open loop system	11	4.04	7.17	2.450
3	Open loop system	10.3	5.92	85.70	0.766
6	Open loop system	6.37	3.09	4.50	2.440

comparative study for the unity feedback system and open loop system with the existence of the PID

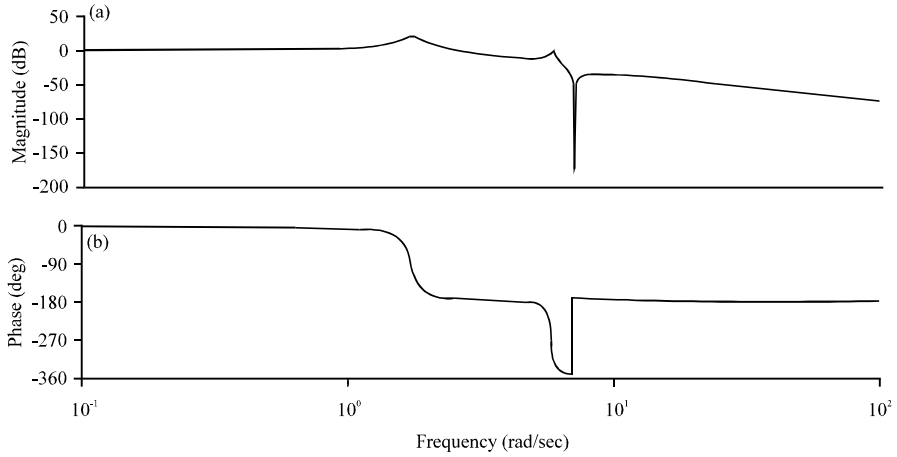

Fig. 18ab): The bode diagram of the open loop system with (K_D = 0)

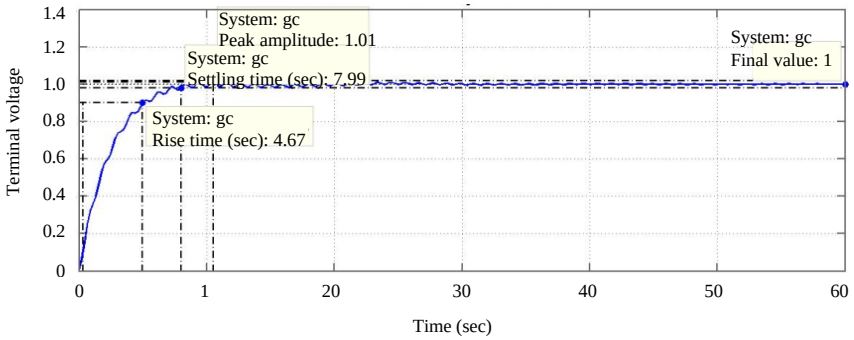

Fig. 19: The step response of the PID controller with system (K_D = 0)

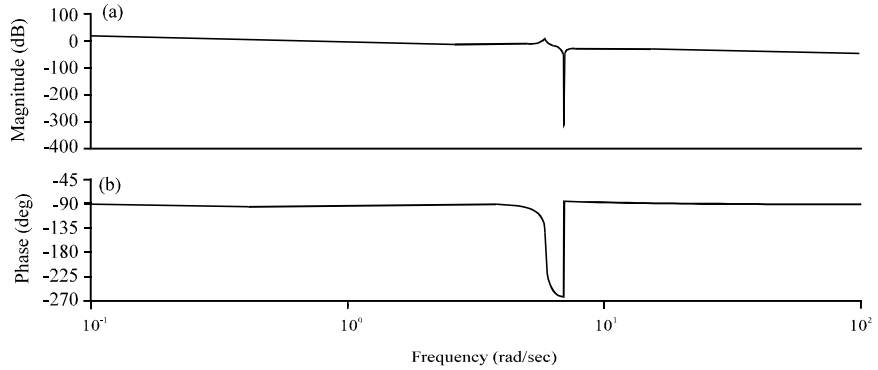

Fig. 20ab): The bode diagram of the PID with system open loop (K_D = 0)

Table 10: The step response performance when applying the PID controller for the three cases of K_D

K_D	Controller types	Peak value	Overshoot (%)	T_r (sec)	T_s(sec)	T_{sse} (sec)
0	System with PID controller	1.01	0.925	4.87	7.99	0
3	System with PID controller	1.01	1.28	2.51	3.82	0
6	System with	1.01	0.574	2.4	3.75	0

controller for the three damping torque coefficient (K_d = 0, K_d = 3 and K_d = 6) are shown in Table 10 and 11.

Table 11: Tthe gain margin and phase margin of the system when applying the PID controller on the open loop for the three values of K_D

K_D	Controller types	Gm (dB)	Wgm (rad/sec)	Pm (degree)	Wpm (rad/sec)
0	Open loop system with PID controller	5.46	5.85	84	0.41
3	Open loop system with PID controller	10.30	5.92	85.7	0.766
6	Open loop system with PID controller	16.50	6.15	86.2	0.85

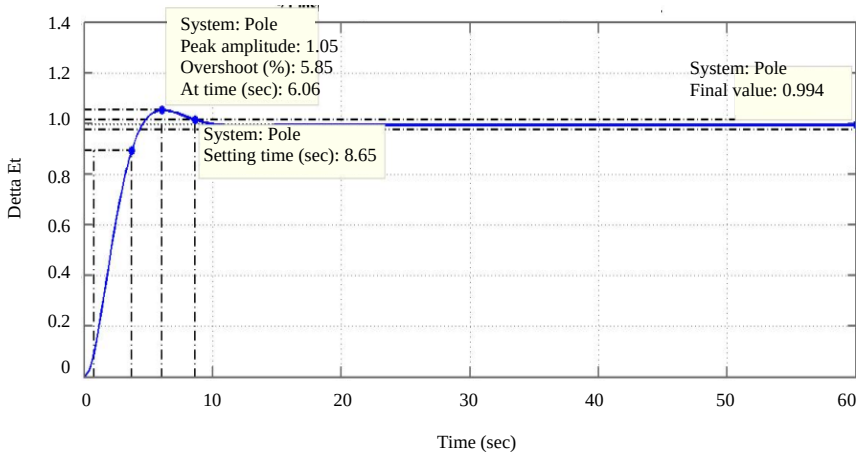

Fig. 21: The pole placement step response ($K_D = 0$)

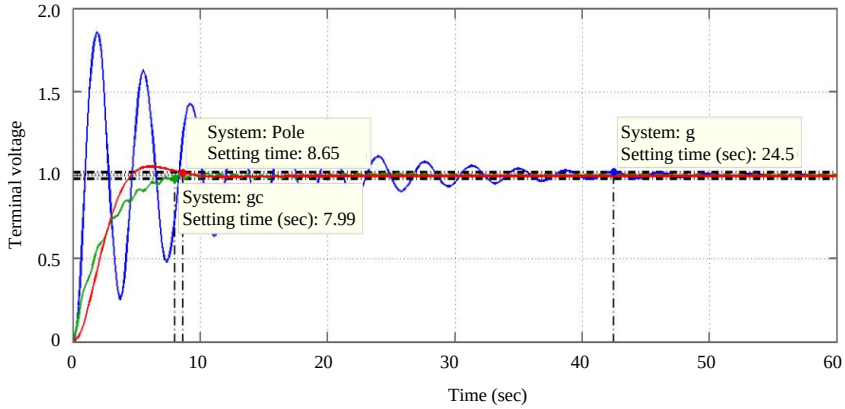

Fig. 22: The three-step responses with ($K_D = 0$)

CONCLUSION

In Fig. 5, when applying the unity feedback as a controller on exciter the step performance are as follows (peak value 1.87, overshoot % 86.8 and settling time 44.6 sec) as given in Table 2. When applying the PID controller with PSO tuning as shown in Fig. 7 the step response performance are as follows (peak value 1.01, overshoot % 1.28 and settling time 3.82 sec) as given in Table 2 and $g_{best} = 0.0204$. In Fig. 9 when applying the pole placement technique the step performance are as follows (peak value 1.05, over shoot % 5.85 and settling time 8.64 sec) as given in Table 2.

In Table 3 it can be seen that, the gain margin and phase margin were the best when applying the PID controller with PSO tuning with the open loop system and when comparing it with the open loop system alone. In standard for a good design the G_m is >6dB and P_m is >40° for the stable system. Also in Fig. 11, it can be seen that the three controllers (unity feedback, PID with PSO tuning and pole placement technique) in which it is proved that the PID controller gives the higher performance than other controllers with $K_D = 3$. When using $K_D = 6$ and made tuning in PSO algorithm to observe the terms of controllers with $g_{best} = 0.0313$, it was seen that all step performances and bode plots will be improved as given in Table 4 and 5 respectively and also shown in Fig. 13 and 14 and it is obvious that its performance better than when applying $K_D = 3$.

When using $K_D = 0$ and made tuning in PSO algorithm to get the terms of the controllers with $g_{best} = 0.0112$, it was seen that all step performances and bode plots less than when comparing it with the other two values of K_D as shown in Table 6 and 7 respectively and also Fig. 19 and 20 with less performance when compared with others K_D. Table 8 and 9 gives the performance of the system without PID controller (peak value, overshoot %, rise time, settling time, gain margin and phase margin) which shows that these performance was less when applying the unity feedback with higher values of K_D. Table 10 and 11 gives the step response results of applying the PID controller (settling time, rise time, over shoot %, gain margin and phase margin) which gives better performances with higher values of K_D except the peak value don't change.

When is taken the K_D value than more 6 the performance of step response is improvement but the gain margin tends to infinity and the stability is high but this is ideal case. It is obvious from the results that the K_D values has direct effect on the PID controller than others controller (unity feedback and pole placement).

Sample data:

- TE = 0.56
- KE = -0.002
- SE = 1.375
- K_1 = 0.7643
- K_2 = 0.8649
- K_3 = 0.323
- K_4 = 1.4187
- K_5 = -0.1463
- K_6 = 0.4168
- KA = 20
- T3 = 2.365
- w_0 = 314
- K_D = 3
- H = 7

List of symbols:

• $_0$	=	Rated speed in elect.rad/sec
•	=	Rotor speed
• • $_r$	=	Speed deviation in pu
• •	=	Rotor angle deviation in elect.rad
KA	=	Regulator gain
T_E	=	Time constant of the exciter
•	=	Rotor angle with respect to infinite bus
H	=	Inertia constant in MW.s/MVA
T_m	=	Mechanical torque in NM
T_e	=	Air-gap torque or electromagnetic torque
K_D	=	Damping torque coefficient
K1-K6	=	Constants

REFERENCES

Andersson, G., 2012. Dynamics and Control of Electric Power Systems. ETH Zurich, Zurich, Switzerland, Pages: 125.

Buelna, C. and R. Soto, 1997. Fuzzy-neuro controller for synchronous generator. Proceedings of the IEEE International Conference on Electric Machines and Drives Record, May 18-21, 1997, IEEE, Milwaukee, Wisconsin, USA., pp: TA2-TA3.

Hasanien, H.M., 2013. Design optimization of PID controller in automatic voltage regulator system using Taguchi combined genetic algorithm method. IEEE. Syst. J., 7: 825-831.

Khalid, A., A.H. Shahid, K. Zeb, A. Ali and A. Haider, 2016. Comparative assessment of classical and adaptive controllers for automatic voltage regulator. Proceedings of the 2016 International Conference on Advanced Mechatronic Systems (ICAMechS'16), November 30-December 3, 2016, IEEE, Melbourne, Australia, ISBN:978-1-5090-5347-6, pp: 538-543.

Krohling, R.A., H. Jaschek and J.P. Rey, 1997. Designing PI/PID controllers for a motion control system based on genetic algorithms. Proceedings of the 1997 IEEE International Symposium on Intelligent Control, July 16-18, 1997, IEEE, Istanbul, Turkey, pp: 125-130.

Kumar, A. and G. Shankar, 2015. Priority based optimization of PID controller for automatic voltage regulator system using gravitational search algorithm. Proceedings of the 2015 International Conference on Recent Developments in Control, Automation and Power Engineering (RDCAPE'15), March 12-13, 2015, IEEE, Noida, India, ISBN:978-1-4799-7247-0, pp: 292-297.

Kundur, P., 1994. Power System Stability and Control. McGraw Hill, New York, USA.

Ogata, K., 2010. Modern Control Engineering. 5th Edn., Prentice-Hall, New Jersey, USA.,.

Puralachetty, M.M., V.K. Pamula and V.N.B. Akula, 2016. Comparison of different optimization algorithms with two stage initialization for PID controller tuning in automatic voltage regulator system. Proceedings of the 2016 IEEE Technology Symposium on Students' (TechSym), September 30-October 2, 2016, IEEE, Kharagpur, India, ISBN:978-1-5090-5164-9, pp: 152-156.

Rao, S.S., 2009. Engineering Optimization Theory and Practice. 4th Edn., John Wiley & Sons, Hoboken, New Jersey, USA., ISBN:978-0-470-18352-6, Pages: 814.

Tuaimah, F.M., N.M. Al-Rawi and W.A. Mahmoud, 2014. Steam turbine governor design based on pole placement technique. Intl. J. Comput. Appl., 92: 51-55.

Verma, S.K., S. Yadav and S.K. Nagar, 2015. Controlling of an automatic voltage regulator using optimum integer and fractional order PID controller. Proceedings of the 2015 IEEE Workshop on Computational Intelligence: Theories, Applications and Future Directions (WCI'15), December 14-17, 2015, IEEE, Kanpur, India, ISBN:978-1-4673-8215-1, pp: 1-5.

Yegireddy, N.K., S. Panda, P. Tentu and K. Durgamalleswarao, 2015. Comparative analysis of PID controller for an automatic voltage regulator system. Proceedings of the International Conference on Electrical, Electronics, Signals, Communication and Optimization (EESCO'15), January 24-25, 2015, IEEE, Visakhapatnam, India, ISBN:978-1-4799-7676-8, pp: 1-6.